

Analysis of narrow terahertz microstrip transmission-line on multilayered substrate

Kumud Ranjan Jha · G. Singh

Published online: 27 October 2010
© Springer Science+Business Media LLC 2010

Abstract In this paper, numerical analysis of the narrow microstrip transmission-line on two and three layer-substrate material at 0.5–1.0 THz frequency of the electromagnetic spectrum is presented. Various analytical results are compared with simulations which have been performed by commercially available simulators: (a) CST Microwave Studio based on the finite integral technique and (b) Ansoft HFSS based on the finite element technique. The proposed narrow microstrip transmission line with improved performance is useful as interconnect for multilayer planar components designed in the terahertz frequency regime of the electromagnetic spectrum. The analysis of the proposed structure has been validated with various reported literature.

Keywords Narrow microstrip-line · Effective permittivity · Multilayer-substrate · Characteristic impedance · Losses · Terahertz antenna

1 Introduction

Due to the increasing demand of the high-speed devices and wideband communication appliances, the bandwidth enhancement is a potential requirement. Terahertz technology

is considered as one of the potential method to solve this problem [1]. The location of terahertz regime of the electromagnetic spectrum from 0.1 to 10 THz, which lies in between the electronics and photonics domains implies that the optical, electronic, or the mixture of optical and electronic techniques can be used for its generation, detection and processing. Compared with the microwave and photonic regime of the spectrum, the terahertz region is not so familiar to various researchers and has remained as terahertz gap in the electromagnetic spectrum since long time. With the advancement in the semiconductor physics and technology, it has attracted attention of scientists and researchers to explore its potential applications in the field of biological imaging and sensing, detection of explosive, spectroscopy and high speed wireless communication [2–7]. For these applications and realization of the practical systems, the fundamental components including antennas, transmission lines, filters, switches, modulators and polarizer are indispensable. In particular, the narrow transmission-line is crucial for the terahertz communication and multispectral imaging. Thus, due to the growing importance and technical breakthrough, various terahertz devices like sources, detectors and antennas are being reported to work efficiently in this frequency regime [8–12].

To convey the electromagnetic energy from one point to the other at terahertz frequency in aforementioned devices, one or other form of the microstrip transmission-line is frequently used [13, 14]. Recently, due to the high demand of system-on-chip/network-on-chip, the multilayer substrate material has gained popularity. Apart from this, the microwave and terahertz antenna geometry on multilayer-substrate has also received a great deal of interest to control the radiation property and impedance bandwidth [15–17] where the microstrip transmission-line is used to excite these antennas. With an increase in the number of substrate layers,

K.R. Jha
School of Electronics and Communication Engineering,
Shri Mata Vaishno Devi University, Katra,
Jammu and Kashmir 182301, India
e-mail: jhkr@rediffmail.com

G. Singh (✉)
Department of Electronics and Communication Engineering,
Jaypee University of Information Technology, Solan 173215,
India
e-mail: drghanshyam.singh@yahoo.com

the substrate thickness is also increased and the propagation characteristic is governed by the order of the substrate layers in between the ground plane and conducting strip-line of the transmission-line.

At the terahertz frequency, the propagation characteristic is the frequency dependent which needs to be explored. On the way to explore the propagation characteristics of a narrow microstrip transmission-line, this paper is motivated to develop a Quasi-TEM formula which is used to analyze the narrow microstrip transmission-line on the multilayer substrates at the submillimeter wavelength. The organization of the paper is as follow. Section 2 concerns with the effective dielectric permittivity of the multi-layered substrate material. In Sect. 3, the results of the frequency dependent effective dielectric permittivity has been compared with simulation and validated with reported literature. Section 4 discusses various kinds of losses to show the potential advantage of multi-layer substrate microstrip transmission-line over the conventional microstrip transmission-line at terahertz regime of the spectrum. Finally, Sect. 5 concludes the work.

2 Effective dielectric permittivity expression

Design of any passive component at the microwave/terahertz frequency begins with the selection of suitable substrate material and the analysis of an effective dielectric permittivity of the material. In general, the multilayer substrate is represented by series capacitance model [18, 19]. The accuracy of this model decreases with the increase in the operating frequency and the number of substrate layers due to dispersive behavior of the substrate materials. Frequency-dependent effective dielectric permittivity of two-layer substrate material is calculated using a new expression [20] which is based on the integrated approach dealt separately in [21–23] which is restricted to the two-layer substrates material only. The schematic diagram of a multilayer substrate material microstrip transmission-line is shown in Fig. 1.

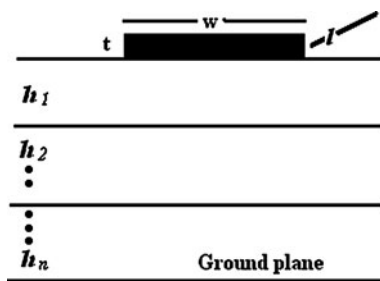


Fig. 1 Schematic of the multi-layer narrow microstrip transmission-line at terahertz frequency

To extend the analysis of the two-layered-substrate material microstrip transmission line to the multilayered-substrate material microstrip transmission-line, the formula presented in [20, 21] is modified as:

$$\epsilon_{rc} = \frac{|d_1| + |d_2| + \dots + |d_n|}{|\frac{d_1}{\epsilon_1}| + |\frac{d_2}{\epsilon_2}| + \dots + |\frac{d_n}{\epsilon_n}|}$$

$$\text{for } h_1 + h_2 + \dots + h_n \cong \lambda_0/10 \tag{1}$$

where

$$d_1 = \frac{K(k_1)}{K'(k_1)} \tag{2}$$

$$d_2 = \frac{K(k_2)}{K'(k_2)} - \frac{K(k_1)}{K'(k_1)} \tag{3}$$

$$d_3 = \frac{K(k_3)}{K'(k_3)} - \frac{K(k_2)}{K'(k_2)} - \frac{K(k_1)}{K'(k_1)} \tag{4}$$

$$d_n = \frac{K(k_n)}{K'(k_n)} - \frac{K(k_{n-1})}{K'(k_{n-1})} - \dots - \frac{K(k_1)}{K'(k_1)} \tag{5}$$

and in general,

$$k_n = \frac{1}{\cosh(\frac{\pi w}{4(h_n+h_{n-1}+h_{n-2}+\dots+h_1)})}$$

for $k = 1, 2, \dots, n$ (6)

In the above equations, h_1, h_2, \dots, h_n are the substrate thicknesses of different layers starting from the top (below the conducting strip of the microstrip transmission-line). In the above equations, the $\epsilon_1, \epsilon_2, \dots, \epsilon_n$ are the complex relative dielectric permittivity of the respective substrate layers and w represents the width of the line. The value of $\frac{K(k)}{K'(k)}$ is calculated by using following formula [24]

$$\frac{K(k_n)}{K'(k_n)} = \frac{1}{\pi} \ln\left(2 \frac{1 + \sqrt{k_n}}{1 - \sqrt{k_n}}\right) \text{ for } 0.7 \leq k_n \leq 1 \tag{7}$$

By using (1) to (7), the frequency-independent relative dielectric permittivity of the multilayer-substrate material (ϵ_{rc}) is obtained. After calculating the frequency-independent relative dielectric permittivity of the multilayer substrate, the frequency dependent relative dielectric permittivity is obtained by using following expressions [22, 23]

$$\epsilon_e(f) = \epsilon_{rc} - \frac{\epsilon_{rc} - \epsilon_e(0)}{1 + (f/f_a)^m} \tag{8}$$

where

$$\begin{aligned}
 f_a &= \frac{f_b}{0.75 + (0.75 - 0.332\varepsilon_{rc}^{-1.73})w/h} \\
 f_b &= \frac{47.746}{h\sqrt{\varepsilon_{rc} - \varepsilon_e(0)}} \tan^{-1} \varepsilon_{rc} \sqrt{\frac{\varepsilon_e(0) - 1}{\varepsilon_{rc} - \varepsilon_e(0)}} \\
 m &= m_0 m_c \\
 m_0 &= 1 + \frac{1}{1 + \sqrt{\frac{w}{h}}} + 0.32(1 + \sqrt{w/h})^{-3} \\
 m_c &= \begin{cases} 1 + \frac{1.4}{1+w/h}(0.15 - 0.235e^{-0.45f/f_a}) & \text{for } w/h \leq 0.7 \\ 1 & \text{for } w/h > 0.7 \end{cases} \quad (9) \\
 \varepsilon_e(0) &= \frac{\varepsilon_{rc} + 1}{2} + \frac{\varepsilon_{rc} - 1}{2} \left(1 + \frac{12h}{w}\right)^{-1/2} + F(\varepsilon_{rc}, h) \\
 &\quad - 0.217(\varepsilon_{rc} - 1) \frac{t}{\sqrt{wh}} \\
 F(\varepsilon_{rc}, h) &= \begin{cases} 0.02(\varepsilon_{rc} - 1)(1 - w/h)^2 & \text{for } w/h < 1 \\ 0 & \text{for } w/h \geq 1 \end{cases}
 \end{aligned}$$

In the above equations, $h = h_1 + h_2 + h_3$, w , and t are the total substrate thickness, width of the transmission-line and the thickness of the conductor, respectively. Here, it is important to mention the reason to consider the absolute value of the parameters in (1). For the three or more substrate layers, the value of d_n as shown in (4) and (5) may be negative. However, its value should remain positive to represent the distance between two parallel plates of the equivalent capacitance model of the substrate. To overcome this limitation, the absolute value of d_n has been used in (1). In addition to this, to follow the quasi-TEM characteristics, the substrate thickness must be smaller than the operating wavelength. On this way, we restrict the total substrate thickness to approximately equal to $\lambda_0/10$.

3 Analysis of the effective dielectric permittivity and characteristic impedance

3.1 Effective dielectric permittivity

To validate the expression presented in the Sect. 2, we have analyzed the frequency-dependent effective dielectric permittivity of a two- and three-layer substrate material narrow microstrip transmission-line. We have arbitrarily selected a three-layer microstrip transmission-line as the schematic of the n-layer substrate material narrow microstrip transmission-line is shown in Fig. 1. The width w and length l of the proposed conducting strip of the microstrip transmission-line are 20 μm and

1000 μm , respectively. The substrate materials of the microstrip transmission-line are arranged in the following manner. The first substrate layer below the conducting strip-line has height $h_1 = 5 \mu\text{m}$, relative dielectric permittivity $\varepsilon_1 = 6.15$, and $\tan \delta = 0.0025$. A substrate material of thickness $h_2 = 40 \mu\text{m}$, relative permittivity $\varepsilon_2 = 2.2$, and $\tan \delta = 0.0009$ follows this layer. The substrate layer above the ground plane is made of thickness $h_3 = 5 \mu\text{m}$, the relative dielectric permittivity $\varepsilon_3 = 2.45$ and $\tan \delta = 0.0019$. The surface area of substrate and ground plane is $1000 \times 400 \mu\text{m}^2$. The microstrip-line and ground plane are made of copper of thickness $t = 20 \mu\text{m}$ each. To compare the analysis, the structure has been simulated by using: CST Microwave Studio and Ansoft HFSS. To maintain the accuracy of the simulation in CST Microwave Studio, the computational region has been increased to 500 μm which is 10 times the total substrate thickness. The computation region is filled with vacuum to take in to the account of fringing field. The structure and computational region are surrounded by the perfect electrical boundaries. The number of perfect boundary approximation (PBA) mesh cells have been increased to 12,89,600. The transmission line is exited by the wave-port of 250 μm height and 400 μm width which are $5h$ and $20w$, respectively. The structure has been simulated in the time-domain transient solver and an effective dielectric permittivity has been obtained from the port information. However, in the Ansoft HFSS, which is based on the finite element method, 13,232 tetrahedral cells have been used. The analytical and simulated value of the effective dielectric permittivity of the three-layer substrate material is shown in Fig. 2.

To validate the expression, we have considered two-layer substrate microstrip transmission-line by choosing the value of $n = 2$. On this way, the third substrate layer (h_3) and relative dielectric permittivity (ε_3) as mentioned in (1)–(7) have been set equal to zero. The total substrate thickness in the present case is 45 μm and other parameters are unchanged. The analytical value of the frequency-dependent effective dielectric permittivity of the two-layer-substrate material along with the simulated results is shown in Fig. 3. From Fig. 2 and Fig. 3, it is revealed that the analytical and simulated results are comparable. The maximum deviation occurs in the case of CST Microwave Studio Simulation. However, the maximum relative error for three-layered and two-layered-substrate microstrip transmission line is about 0.98% and 1.2%, respectively. It is worthy to mention here that the presented result in this manuscript shows improvement in the accuracy of effective dielectric permittivity in comparison to our recently reported work [20]. Apart from this, there is the significant improvement in the accuracy of the present model in comparison to [25] at 1000 GHz.

Fig. 2 Frequency dependent an effective dielectric permittivity of the three-layer substrate materials narrow microstrip transmission-line

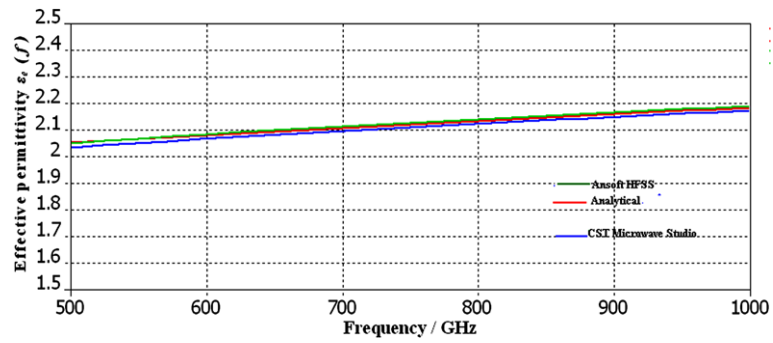
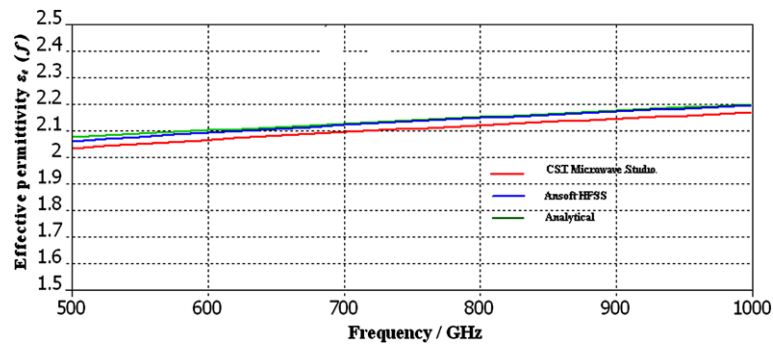


Fig. 3 Frequency dependent an effective dielectric permittivity of the two-layer substrate material narrow microstrip transmission-line



3.2 Characteristic impedance

Due to the dependence of the effective dielectric permittivity on the frequency, the characteristic impedance of the microstrip transmission-line also changes. To examine this effect on the multilayer substrate microstrip transmission-line, we have analyzed the frequency dependent characteristic impedance of the transmission-line in this section. It is seen that the characteristic impedance of the line also increases with the increase in the frequency which is mainly due to the increase in the effective dielectric permittivity of the substrate material. The dispersive behavior of the characteristic impedance on the multilayered substrate material can be predicted by following set of formulas [23, 26].

$$Z_c(f) = Z_c \frac{\epsilon_e(f) - 1}{\epsilon_e(0) - 1} \sqrt{\frac{\epsilon_e(0)}{\epsilon_e(f)}} \tag{10}$$

where

$$Z_c = \frac{120\pi}{2\sqrt{\epsilon_r(0)}} \ln\left(\frac{8h}{w_e} + 0.25\frac{w_e}{h}\right) \text{ for } \frac{w_e}{h} \leq 1 \tag{11}$$

and

$$w_e = \frac{w}{h} + \frac{1.25t}{\pi h} \left(1 + \ln\frac{4\pi w}{t}\right) \text{ for } \frac{w}{h} \leq 0.5\pi \tag{12}$$

To calculate the value of $Z_c(f)$, the value of $\epsilon_e(f)$ and $\epsilon_e(0)$ are obtained from (8) and (9), respectively. The analytical and simulated value of the characteristic impedance for two-layer and three-layer transmission-line is shown in Fig. 4(a)

and (b), respectively. From Fig. 4(a) and (b), it is revealed that the characteristic impedance of the transmission-line increases with the increase in the operating frequency. In both the cases, simulation as well as analytical curve follows the same pattern. The maximum relative error which occurs at 1000 GHz is equal to 2.8% and 6% in the case of two-layer substrate and three-layer substrate microstrip transmission-line, respectively. It indicates that with the increase in the number of substrate layers, this error may increase even though for the same overall substrate thickness. The relative error in the characteristic impedance of two-layer substrate microstrip transmission line is comparable to the relative error reported in [27].

3.3 Effect of the number of substrate layers on the characteristic impedance of the transmission line

From (10), it is seen that the value of $Z_c(f)$ depends on $\epsilon_e(f)$. Moreover, the accuracy of $Z_c(f)$ is dependent on the degree of the accuracy of $\epsilon_e(f)$. In order to check the correctness of the proposed numerical model for the multilayer substrate material microstrip transmission-line, we have applied the presented model in this manuscript on the four-layer and five-layer substrate-material microstrip transmission-line while keeping the overall height of the substrate constant. In both the configurations of the multilayered substrate material, the heights of the various substrate layers are denoted by $h_1, h_2,$ and $h_n,$ respectively. The substrate layer configuration of the four- and five-layered substrate material microstrip-transmission-line is shown in

Fig. 4 Frequency dependent characteristic impedance of the narrow microstrip transmission-line on (a) two layer and (b) three layer substrate material

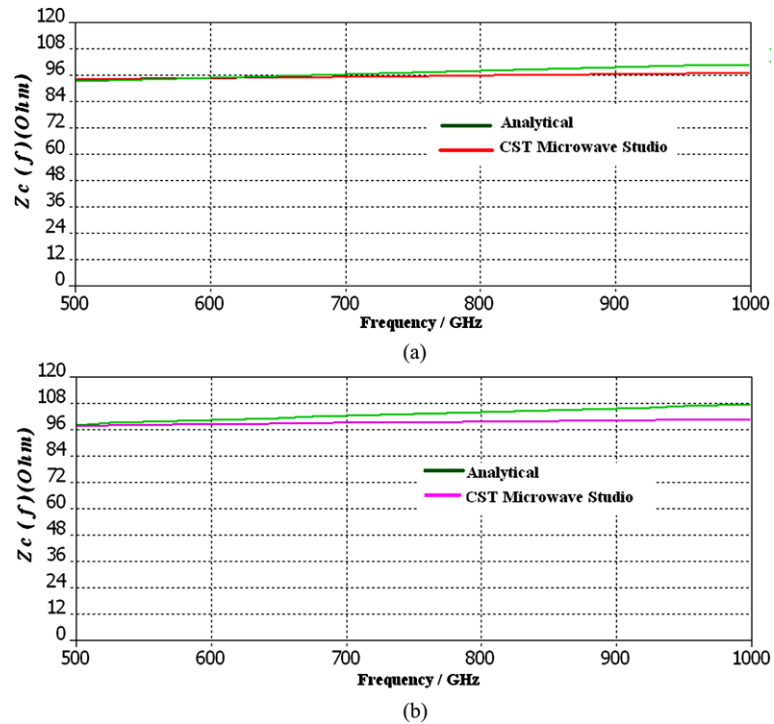


Table 1 Configuration of multi-layer substrate material

Four-layered substrate				Five-layered substrate			
Layer No.	Thickness (μm)	ϵ_r	$\tan \delta$	Layer No.	Thickness (μm)	ϵ_r	$\tan \delta$
h1	10.0	7.0	0.001	h1	10.0	7.0	0.001
h2	5.0	6.15	0.0025	h2	5.0	6.15	0.0025
h3	40.0	2.2	0.0009	h3	20.0	4.5	0.0009
h4	5.0	2.45	0.0019	h4	20.0	2.2	0.0009
				h5	5.0	2.45	0.0019

the Table 1. The total substrate thickness in the both cases is equal to 60 μm. The value of $Z_c(f)$ has been calculated by using (10)–(12). To compare the result, the multilayer substrate structure has also been simulated in CST Microwave Studio and Ansoft HFSS. The results for the four-layered and five-layer substrate are shown in Figs. 5 and 6, respectively.

From Figs. 5 and 6, it is seen that the analytical model closely follows the simulated results achieved by the simulating the structure by using CST Microwave Studio as well as in Ansoft HFSS software. The maximum deviation in the analytical and simulated model occurs at the lower frequency band. The relative maximum deviation of the analytical result in comparison to the simulated results in the four-layer and five-layer substrate structure is 3.16% and 10.7%, respectively. The comparison of the characteristic impedance for two-layer, three-layer, four-layer and five-layer substrate material microstrip transmission-line is

shown in Figs. 4(a), 4(b), 5 and 6, respectively, which indicates that the model can predict the behavior of the microstrip transmission-line correctly up to four-layer substrate material. With an increase in the number of layers above four, the relative error increases to a significant value. However, the error is reduced with the increase in the operating frequency and it indicates the potential application of the presented model at the higher frequency. It is also important to mention that the practical application of the five- and more-layer substrate material is reduced due to the fabrication complexity. In the view of this fact, the proposed model finds a practical application in the analysis and design of the multilayer substrate material microstrip transmission-line.

4 Losses in the microstrip transmission-line

In this section, we have calculated two types of losses (a) dielectric loss and (b) conductor loss. The analysis has been compared with the simulated results obtained by using CST Microwave Studio and Ansoft HFSS simulation.

4.1 Dielectric loss

Here, it is important to note that the effective dielectric permittivity is frequency dependent complex quantity. In the case of multilayer substrate, the loss tangent of composite material is also modified in accordance with the position of substrate layers. The frequency-independent loss tangent of the multilayer transmission line can be obtained by a simple

Fig. 5 The frequency-dependent characteristic impedance of four-layer substrate material narrow microstrip transmission-line

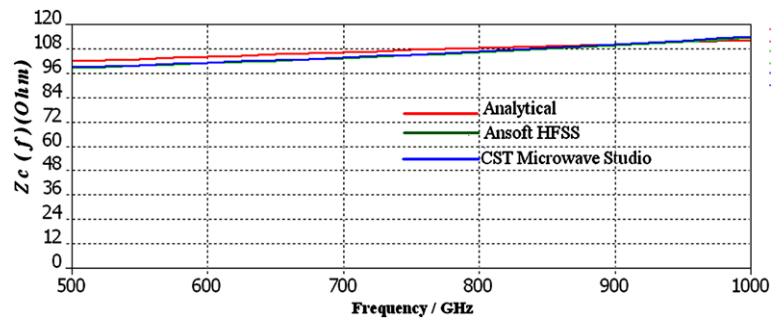
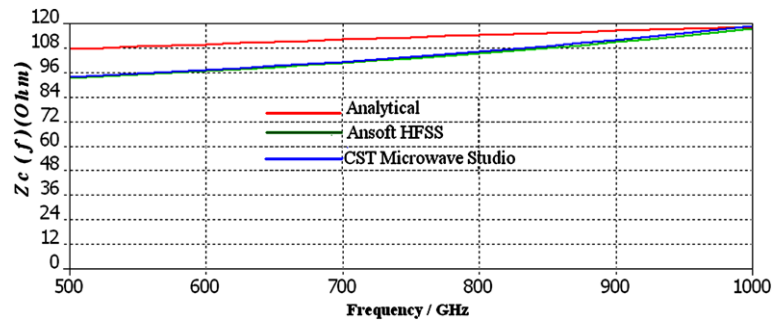


Fig. 6 The frequency-dependent characteristic impedance of five-layered substrate material narrow microstrip transmission-line



series-capacitance-method in which the relative dielectric permittivity of each layer is replaced by its complex value and the equivalent complex relative dielectric permittivity of the substrate layers is calculated. After calculating the value of frequency independent loss tangent, it can be substituted in the following expression to obtain the frequency dependent dielectric attenuation constant $\alpha_d(f)$ of the multilayer substrate material [28, 29]

$$\alpha_d(f) = 8.686\pi \frac{\epsilon_e(f) - 1}{\epsilon_{rc} - 1} \frac{\epsilon_{rc}}{\epsilon_e(f)} \frac{\tan \delta}{\lambda_g} \text{ dB/unit length} \quad (13)$$

In (13), the value of ϵ_{rc} and $\epsilon_e(f)$ are obtained from (1) and (8), respectively. Other variables such as λ_g is the guided wavelength and $\tan \delta$ is obtained from a simple series capacitance model of the multilayer substrate material.

To simulate the dielectric loss in the CST Microwave Studio, we have activated E-field and H-Field monitor at each frequency point of the interest and calculated the dielectric quality factor (Q) of the multilayered-substrate microstrip transmission line by using the loss and quality factor calculation macro. The calculated value of quality factor can be placed in the following formula to obtain the frequency dependent attenuation constant [30]

$$\alpha_d(f) = 8.686\beta/2Q_d \text{ dB/unit length} \quad (14)$$

In (14) β and Q_d are phase constant in dielectric and dielectric quality factor, respectively. Based on (13) and (14), we have calculated the frequency dependent dielectric attenuation constant for the three-layer substrate microstrip transmission-line which was analyzed in the preceding section and the result is presented in Fig. 7.

From Fig. 7, it is revealed that, the dielectric loss also increases with the increase in frequency. Further, it is noticed that the two curves are close to each other at each frequency point.

4.2 Conductor loss

The conductor loss of narrow microstrip line is influenced by the width of metallization and characteristic impedance of the line. However, the characteristic impedance of the line itself is an inconsistent parameter at terahertz frequency, which makes the analysis of conductor loss a challenging task. We have successfully used the formula proposed in [31, 32] to calculate the conductor attenuation constant of a narrow microstrip transmission-line at terahertz frequency

$$\alpha_c(f) = \frac{8.68}{2\pi} \frac{R_s}{Z_c(f)h} \left[1 - \left(\frac{w_e}{4h} \right)^2 \right] \times \left[1 + \frac{h}{w_e} + \frac{h}{w_e} \left(\ln \frac{2h}{t} - \frac{t}{h} \right) \right] \quad (15)$$

for $\frac{1}{2\pi} \leq \frac{w}{h} \leq 2$

where

$$R_s = \sqrt{\frac{\pi f \mu}{\sigma}}$$

In (15), the value of $Z_c(f)$ and w_e have been calculated by using (10) and (12), respectively. To compare the analysis, the conductor attenuation constant has also been simulated by using the CST Microwave Studio. In this case conductor

Fig. 7 Frequency dependent dielectric attenuation constant of the narrow microstrip transmission-line

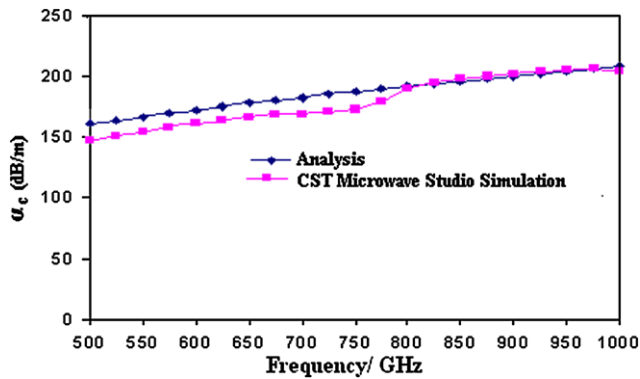
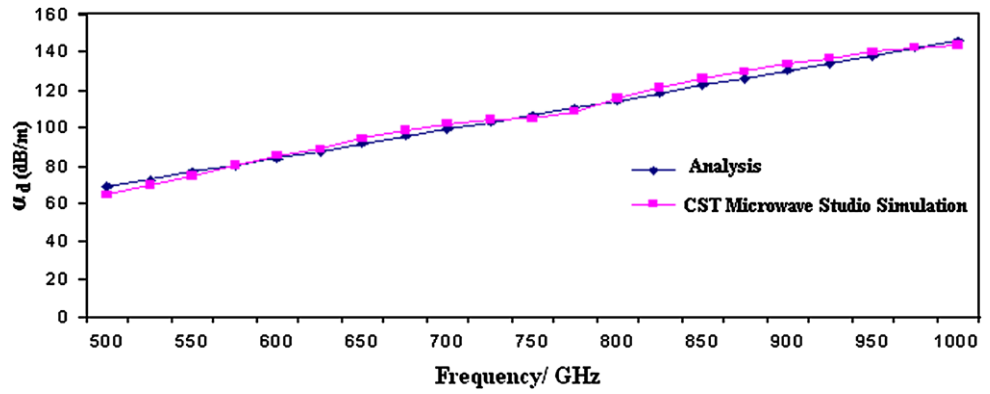


Fig. 8 Frequency dependent conductor attenuation constant of the narrow microstrip transmission-line at terahertz frequency

quality factor (Q_c) has been extracted from the simulation and it has been substituted in (14) in place of Q_d as:

$$\alpha_c(f) = 8.686\beta/2Q_c \text{ dB/ unit length} \tag{16}$$

The resultant conductor attenuation constant obtained by analysis and simulation is shown in Fig. 8.

From Fig. 8, it is seen that simulated as well as analytical attenuation constant curves follow almost the same pattern except a deviation near 750 GHz. The maximum relative error of analysis and simulation is 7% at this frequency. Next to this, total attenuation constant due to the conductor and dielectric loss is shown in Fig. 9.

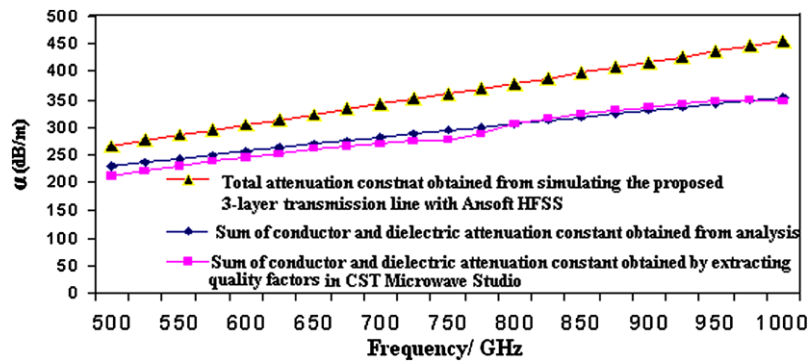
In Fig. 9, the first curve from the bottom shows the sum of the conductor and dielectric attenuation constant obtained by extracting the quality factors by using the CST Microwave Studio. The next curve to this shows the sum of conductor and dielectric attenuation constant obtained from the numerical analysis. The first curve from the top shows the total attenuation when the proposed three-layer substrate microstrip line is simulated by using the Ansoft HFSS. From Fig. 9, it is seen that the sum of conductor and dielectric attenuation constant obtained from analysis and CST Microwave Studio simulation are comparable in the range of 0.5–1.0 THz frequency. However, the radiation

loss has not been considered in these calculations. The Ansoft HFSS simulation (first line from the top of Fig. 9) shows the total loss in the transmission line. From the above analysis, we conclude that the variation between the first curve and second curve from the top indicates other losses. However, the radiation loss is dominant at the high frequency and we conclude that this variation is due to the radiation loss. Further, with an increase in the frequency, the variation between these curves increases and indicates that the radiation loss increases with the increase in the operating frequency. The total loss at 1 THz is 455 dB/m. However, the predicted loss in the multilayer transmission line in this manuscript is smaller than the figure predicted by Yeh et al. [33]. According to them, for the conventional microstrip transmission line, the total attenuation is 150 dB/m at 300 GHz and it increases at the rate of $f^{3/2}$ with the increase in the operating frequency. On this way, the expected attenuation in a conventional microstrip transmission-line at 1 THz is 912 dB/m. However, three-layered transmission-line as presented in this manuscript shows quite more smaller value of the total loss. Further, it is required to mention that the size of the terahertz devices are in the order of micrometer and multilayered-transmission line can serve the purpose of interconnects.

5 Conclusion

In this paper, we have analyzed and simulated a narrow microstrip transmission-line on the two- and three-layer substrate materials at terahertz frequency. The analysis shows that the proposed expressions are useful for the computation of various important characteristics parameters of a narrow microstrip transmission-line up to the four-layered substrate materials at the terahertz frequency. We have compared the results of proposed analysis with simulation by using two commercially available simulators such as CST Microwave Studio and Ansoft HFSS. The analytical results are comparable with the two simulated results. However, the proposed technique is limited by the ratio of $h \cong \lambda_0/10$ and

Fig. 9 Total, conductor, and dielectric attenuation constant of the three layer substrate narrow microstrip transmission-line



$w/h \leq 1$. In this manuscript, the effect of surface roughness of the conductor has not been considered in the analysis and it would be communicated in the near future. In addition to this, the improved analysis of five- and more-layered-substrate microstrip transmission-line would be reported in the due course of the time.

Acknowledgements Authors are thankful to the unanimous reviewers for their valuable comments and suggestions to improve the quality of the manuscript.

References

1. Miles, R., Harrison, P., Lippens, D.: Terahertz Sources and Systems. Kluwer Academic, Norwell (2001)
2. Siegel, P.H.: THz instruments for space. IEEE Trans. Antennas Propag. **55**(11), 2957–2965 (2007)
3. Siegel, P.H.: THz technology in biology and medicine. IEEE Trans. Microw. Theory Tech. **52**(10), 2438–2448 (2004)
4. Galoda, S., Singh, G.: Fighting terrorism with terahertz. IEEE Potentials Mag. **26**(6), 24–29 (2007)
5. Kawase, K., Ogawa, Y., Watanabe, Y.: Non-destructive terahertz imaging of illicit drugs using spectral fingerprints. Opt. Express **11**(20), 2549–2554 (2003)
6. Laskar, J., Princl, S., Dawn, D., Sarkar, S., Perumana, B., Sen, P.: The next wireless wave in millimeter wave. Microw. J. **50**, 23–36 (2007)
7. Piesiewicz, R., Kelvin-Ostmann, T., Krumbholz, N., Mittleman, D., Koch, M., Schoebel, J., Kuner, T.: Short-range ultra broadband terahertz communication: concept and perspectives. IEEE Antennas Propag. Mag. **49**(6), 24–39 (2007)
8. Fitch, M.J., Ostiander, R.: Terahertz waves for communications and sensing. John Hopkins APL Technical Dig. **25**(4), 348–355 (2004)
9. Sharma, A., Singh, G.: Rectangular microstrip patch antenna design at THz frequency for short-distance wireless communication. J. Infrared Millim. Terahertz Waves **30**(1), 1–7 (2009)
10. Singh, G.: Design consideration for rectangular microstrip patch antenna on electromagnetic crystal substrate at terahertz frequency. Infrared Phys. Technol. **53**(1), 17–22 (2010)
11. Shimiza, N., Nagastuma, T.: Photodiode-integrated microstrip antenna array for sub-terahertz radiation. IEEE Photonic Technol. Lett. **18**(6), 743–746 (2006)
12. Maki, K., Otani, C.: Terahertz beam steering and frequency tuning by using spatial dispersion of ultra-fast laser pulses. Opt. Express **16**(14), 10158–10169 (2008)

13. Koday, Y., Onuma, M., Yanagi, S., Ohkubo, T., Sato, N., Kitagawa, J.: THz wave propagation on strip-lines: devices, properties, and applications. Radioengineering **17**(2), 48–55 (2008)
14. Treizebra, A., Bocquet, B., Xu, Y., Bosisio, R.G.: New THz excitation of planar Goubau line. Microw. Opt. Technol. Lett. **50**(11), 2998–3001 (2008)
15. Sharma, A., Singh, G.: Design of single pin shorted three-dielectric-layered substrates rectangular patch microstrip antenna for communication systems. Prog. Electromagn. Res. Lett. **2**, 157–167 (2008)
16. Ghassemi, N., Rashed-Mohassel, J., Neshati, M.H., Tavakoli, S., Ghaaemi, M.: High gain dual stacked aperture coupled microstrip antenna for wideband applications. Prog. Electromagn. Res. B **9**, 125–135 (2009)
17. Sharma, A., Singh, G., Chauhan, D.S.: Design considerations to improve the performance of a rectangular microstrip patch antenna at THz frequency. In: Proc. 33rd Int. Conf. on Infrared, Millimeter and Terahertz Waves, IRMMW-THz 2008, Pasadena, CA, 15–19 Sept. 2008, pp. 1–2 (2008)
18. Jha, K.R., Singh, G.: Dual-band rectangular microstrip patch antenna at terahertz frequency for surveillance system. J. Comput. Electron. **9**(1), 31–41 (2010)
19. Iskander, M.F.: Electromagnetic Fields and Waves. Prentice-Hall, New York (1992)
20. Jha, K.R., Singh, G.: Analysis and design of rectangular microstrip antenna on two-layer substrate materials at terahertz frequency. J. Comput. Electron. **9**(2), 68–78 (2010)
21. Yoon, Y.J., Kim, B.: New formula for effective dielectric constant in multi-dielectric layer microstrip structure. In: IEEE Conf. on Electrical Performance of Electronic Packaging, Scotsdale, AZ, Oct. 23–25, 2000, pp. 163–167 (2000)
22. Kobayshi, M.: A dispersive formula satisfying recent requirements in microstrip CAD. IEEE Trans. Microw. Theory Tech. **36**(8), 1246–1250 (1988)
23. Hammerstad, E.O., Jensen, O.: Accurate models for microstrip computer-aided design. In: Proc. IEEE MTT-S Digest, pp. 407–409 (1980)
24. Collin, R.E.: Foundation for Microwave Engineering, 2nd edn. McGraw-Hill, New York (1992)
25. Heiliger, H.M., Nagel, M., Roskos, H.G., Kurz, H., Schnieder, F., Heinrich, W.: Thin-film microstrip lines for mm and sub-mm wave on-chip interconnects. IEEE Int. Microw. Symp. Dig. **2**, 421–424 (1997)
26. Bahl, I.J., Garg, R.: Simple and accurate formula for microstrip with finite strip thickness. Proc. IEEE **65**, 1611–1612 (1977)
27. Schnieder, F., Heinrich, W.: Model of thin-film microstrip line for circuit design. IEEE Trans. Microw. Theory Tech. **49**(1), 104–110 (2001)
28. Monsour, R.R., Jolley, B., Ye, S., Thomsan, F.S., Dokas, V.: On the power handling capacity of high temperature superconductive filters. IEEE Trans. Microw. Theory Tech. **44**(7), 1322–1338 (1996)

29. Hong, J.-S., Lancaster, M.J.: Microstrip triangular patch resonator filters. In: Proc. IEEE MTT-S Dig., vol. 1, pp. 331–334 (2000)
30. Kapilevich, B., Faingersh, A., Gover, A.: Accurate determination of Q factors of a quasi-optical resonator. *Microw. Opt. Technol. Lett.* **35**(4), 303–306 (2003)
31. Pucel, R.A., Masse, D.J., Hartwig, C.P.: Losses in microstrip. *IEEE Trans. Microw. Theory Tech.* **16**(6), 342–350 (1968)
32. Pucel, R.A., Masse, D.J., Hartwig, C.P.: Correction to losses in Microstrip. *IEEE Trans. Microw. Theory Techn.* **16**(12), 1064 (1968)
33. Yeh, C., Shimabukuro, F., Siegel, P.H.: Low-loss terahertz ribbon waveguides. *Appl. Opt.* **44**(28), 5937–5946 (2005)